Mechanical and biological properties of nanoporous carbon membranes

2008 Biomed. Mater. 3 034107

(http://iopscience.iop.org/1748-605X/3/3/034107)

Biomed. Mater. **3** (2008) 034107 (7pp) doi:10.1088/1748-6041/3/3/034107

Mechanical and biological properties of nanoporous carbon membranes

Roger J Narayan[1], Ravi Aggarwal[1], Wei Wei[1], Chunming Jin[1], Nancy A Monteiro-Riviere[1,2], Rene Crombez[3] and Weidian Shen[3]

[1] Joint Department of Biomedical Engineering, University of North Carolina, Chapel Hill, NC 27599-7575, USA
[2] Center for Chemical Toxicology Research and Pharmacokinetics, North Carolina State University, Raleigh, NC 27695, USA
[3] Surface Science and Nano-Tribology Laboratory, Eastern Michigan University, Ypsilanti, MI 48197, USA

E-mail: roger_narayan@unc.edu

Received 14 January 2008
Accepted for publication 28 March 2008
Published 8 August 2008
Online at stacks.iop.org/BMM/3/034107

Abstract
Implantable blood glucose sensors have inadequate membrane–tissue interfaces for long term use. Biofouling and inflammation processes restrict biosensor membrane stability. An ideal biosensor membrane material must prevent protein adsorption and exhibit cell compatibility. In addition, a membrane must exhibit high porosity and low thickness in order to allow the biosensor to respond to analyte fluctuations. In this study, the structural, mechanical and biological properties of nanoporous alumina membranes coated with diamond-like carbon thin films were examined using scanning probe microscopy, nanoindentation and MTT viability assay. We anticipate that this novel membrane material could find use in immunoisolation devices, kidney dialysis membranes and other medical devices encountering biocompatibility issues that limit *in vivo* function.

(Some figures in this article are in colour only in the electronic version)

Introduction

Conventional implantable blood glucose sensors exhibit poor *in vivo* performance. Biofouling and tissue encapsulation create barriers that decrease the transport of analytes between the sensor and the surrounding tissues [1]. These biocompatibility issues have been far more challenging than electrode passivation, electrical failure, enzyme degradation or other biosensor-related issues. Biofouling is the buildup of cells, proteins and other materials on an implant surface. This phenomenon starts immediately after implantation, when $<$3 kDa proteins undergo adhesion and adsorption processes on the implant surface [2]. In some cases, biological molecules and cells may obstruct pores and other features on the implant surface. The thickness of the biofouling layers can vary between 20 and 0.5 μm [3]. *In vivo* and *in vitro* studies have shown that membrane biofouling results in decreased biosensor signal strength [4, 5].

Several materials, including Nafion®, hydrogels, phospholipids and surfactants, have been utilized to modulate the tissue–material interface of implantable biosensor materials. The goal of these materials is to maintain the passage of analyte molecules between the biosensor and the surrounding tissues over an extended period of time. Specifically, biosensor membrane materials exhibit low protein adsorption and high cell compatibility. Furthermore, these membranes must be thin and porous in order to allow the biosensor to rapidly respond to analyte concentration changes. Polymeric materials have generally not been successful in maintaining a permeable *in vivo* biosensor interface. Novel biosensor membrane materials must be developed that exhibit low levels of biofouling and good cell compatibility.

Recently, nanoporous materials have been considered for use as biosensor membranes. Ion-track etching has been used to form nanoporous membranes, and these materials are now widely available (e.g., Millipore Isopore™). The

ion-track etching technique produces relatively thin materials (thickness between 7 and 22 μm) with a relatively tight pore size distribution (pore variation within 10%). Unfortunately, ion-track etched membranes exhibit relatively low porosity values; pore concentration values under 10^9 pores cm^{-2} are typically observed. Porous silicon is another material that has been considered as biosensor membrane material. This material is fabricated by electrochemically corroding silicon in a hydrofluoric acid solution. The pores propagate in the $\langle 1\,0\,0\rangle$ direction of the silicon crystal. The average diameter of the nanocrystalline porous silicon layers can be modulated using appropriate electrolyte composition, electrochemical current or wafer dopant parameters [6]. Unfortunately, porous silicon may undergo fouling (e.g., calcium phosphate mineralization) and biofouling within hours of implantation [7]. In addition, porous silicon materials undergo biological degradation under physiologic conditions; in fact, porous silicon may be appropriately suited for use as a biodegradable drug delivery scaffold [8].

Narayan *et al* developed diamond-like carbon-coated nanoporous alumina for use as a potential biosensor membrane material [9]. Prolonged anodization of aluminum, stripping of the aluminum oxide layer and re-anodization produces a nanoporous material [10]. Nanoscale pores are randomly formed on the aluminum oxide surface during anodization. Then these pores self-organize into a hexagonal configuration during growth into the bulk material. This first oxide layer is typically removed using an aqueous solution of 1.8 wt% Cr (VI) oxide and 6 wt% phosphoric acid. Nanoporous alumina is relatively thin ($\sim$60 μm), and contains high density, long, columnar, ordered nanoscale pores. This material provides several advantages over conventional materials as a sensor membrane. These membranes can be processed with smaller pore sizes (10–100 nm range), more uniform pore sizes and lower membrane thicknesses (5 μm range) than polymer membranes. Finally, the anodization process provides precise control over pore size and distribution.

Diamond-like carbon (DLC) is an ideal interface between the biosensor and the surrounding biological environment. The term diamond-like carbon is used to describe amorphous carbon materials that possess a significant fraction of sp^3 hybridized carbon atoms [11–16]. In a previous study, we have demonstrated that diamond-like carbon-coated nanoporous alumina membranes remained free from fibrin networks or platelet aggregation after exposure to platelet rich plasma [9]. A few small, widely scattered crystals were observed on the film surface. The presence of sodium and chlorine within the energy dispersive x-ray analysis spectra for platelet rich plasma-exposed nanoporous alumina membranes suggest that the sodium chloride crystals precipitate from the platelet rich plasma. The clotting process has been attributed to a charge transfer theory, in which an exchange of electrons between blood proteins and the surface of a material initiates the release of fibrinopeptides that cause thrombosis [17]. The rate of charge transfer during the interaction of platelet rich plasma and the medical device surface is a function of the time constant of the material. The time constant for diamond-like carbon is significantly higher than those for thrombogenic metal-containing materials. As a result, the diamond-like carbon film exhibits a lower amount of charge transfer. Studies by other investigators have shown that platelet activation and platelet adhesion occur less often on diamond-like carbon-coated surfaces than on titanium, titanium carbide, titanium nitride and stainless steel surfaces [18–21]. Jones *et al* have suggested that the extremely low surface energies (40–44 mN m^{-1}) and large contact angles (75–80° with water) exhibited by diamond-like carbon prevent fouling by proteins [20]. Ultraviolet pulsed laser deposition will be used to produce hydrogen-free diamond-like carbon thin films with a high fraction of sp^3 hybridized carbon atoms. Pulsed laser deposition of diamond-like carbon is a physical vapor deposition process, in which a sp^2-hybridized carbon target (e.g., graphite) is ablated at room temperature and under high vacuum. The advantages of pulsed laser deposition are fast deposition times, nonequilibrium depositing species and room temperature deposition.

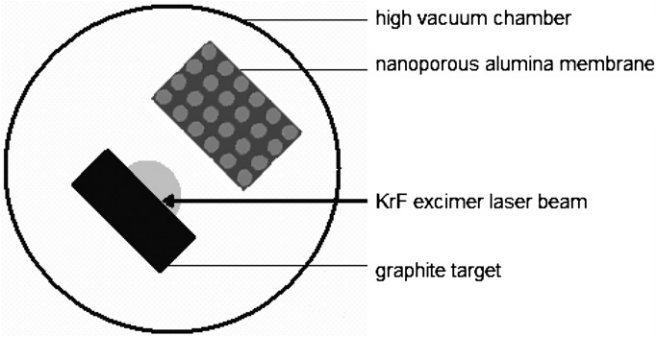

Figure 1. Schematic of pulsed laser deposition system used for deposition of diamond-like carbon thin films.

In this study, the structural, mechanical and biological properties of nanoporous alumina membranes coated with diamond-like carbon thin films were examined using scanning probe microscopy, nanoindentation, and MTT cell viability or cytotoxicity assay. We anticipate that this novel membrane material could be used in immunoisolation devices, kidney dialysis membranes and other medical devices that face biocompatibility issues.

Experimental procedure

100 nm pore diameter nanoporous alumina membranes were obtained from a commercial source (Whatman, Brentford, UK). The membranes have thickness of $\sim$60 μm and porosity values between 25% and 50%. Ultraviolet pulsed laser deposition was used to deposit hydrogen-free diamond-like carbon thin films, gold films, titanium films on nanoporous alumina membranes (figure 1). A Compex 205 KrF excimer laser (Coherent, Fort Lauderdale, FL) operating at $\lambda = 248$ nm was used for ablation of the graphite, titanium or gold target. The target materials were supplied by a commercial source (Alfa Aesar, Ward Hill, MA, USA). The substrates and targets were loaded into a high vacuum chamber, which was evacuated to a base pressure of $\sim 1 \times 10^{-4}$ Pa. The target–substrate distance was maintained at 4.5 cm. The laser was operated

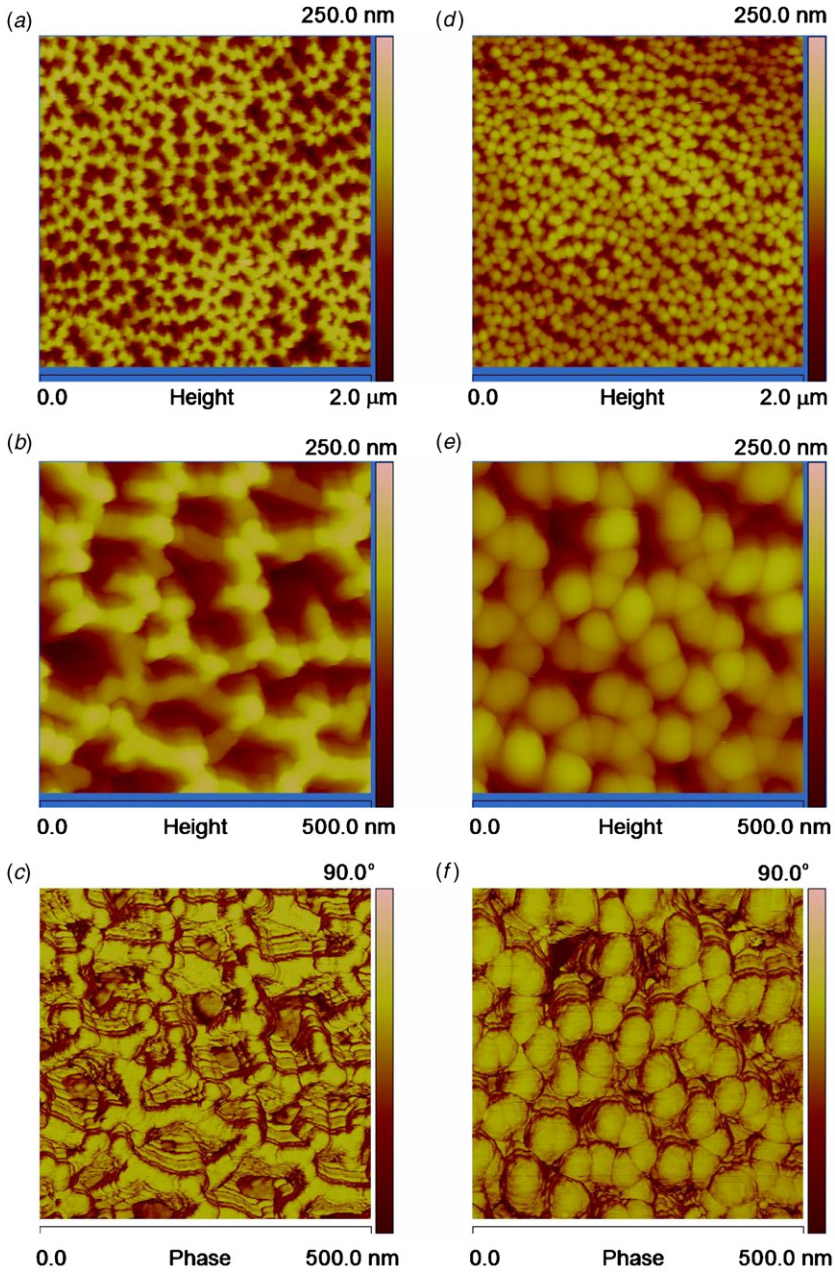

Figure 2. (*a*) 2 μm × 2 μm topographic image of as-prepared 100 nm pore size membrane. (*b*) 500 nm × 500 nm topographic image of as-prepared 100 nm pore size membrane. (*c*) Phase image of as-prepared 100 nm pore size membrane. (*d*) 2 μm × 2 μm topographic image of DLC-coated 100 nm pore size membrane. (*e*) 500 nm × 500 nm topographic image of DLC-coated 100 nm pore size membrane. (*f*) Phase image of DLC-coated 100 nm pore size membrane.

using a frequency of 10 Hz and a pulse duration of 25 ns. A laser energy output of 215 mJ and a laser spot size of 0.04 cm^2 were employed in these experiments. The average energy density was maintained at ∼5 J cm^{-2}. The target was rotated at a rate of 5 rpm during the deposition process. The substrate was placed at an angle of 45° with respect to the target. Diamond-like carbon films, gold films and titanium films were deposited on the nanoporous alumina membranes at 25 °C for 2 min. Previous profilometry studies suggest that diamond-like carbon films prepared with similar deposition conditions exhibit film thicknesses of ∼12 nm [14]. In our previous work, we have shown that pulsed laser deposition using similar deposition conditions produces diamond-like carbon that contain 44% tetrahedrally hybridized carbon atoms [9].

The pore size, pore structure, pore density and surface topology of the as-prepared (uncoated) and diamond-like carbon-coated nanoporous alumina membranes were examined with a nanoscope IIIa scanning probe microscope (Veeco Instruments, Santa Barbara, CA, USA), which was operated in the tapping mode. Indentation studies were carried out using a nano-indenter XP system (MTS Nano Instruments, Oak Ridge, TN, USA) with a three-sided pyramidal Berkovich diamond tip. Studies were performed at six sites on each

sample with spacing between sites greater than 250 μm. Each test consisted of 13 maximum load cycles, from 0.1 mN up to 409.6 mN, doubling the load after each cycle. The chemical composition of the diamond-like carbon-coated nanoporous alumina membrane was assessed using an LAS-3000 x-ray photoelectron spectrometer (Riber, Rueil-Malmaison, France) with a Mg Kα source ($\lambda = 1254$ eV) and a 1 mm spot size. The take-off angle was 75° from the surface; the x-ray incidence angle was 20°; and the x-ray source-analyzer angle was 55°. The base pressure in the analysis chamber was approximately 1×10^{-8} Pa.

Cryopreserved neonatal human epidermal keratinocytes (HEK) were purchased from a commercial source (Lonza, Basel, Switzerland). HEK were plated in 6-well culture plates at density of approximately 100 000 HEK in 3 ml of KGM-2 media. Cells were grown in a humidified environment of 5% CO_2 at 37 °C. Cells were maintained in keratinocyte growth media (KGM-2), consisting of serum-free keratinocyte basal media supplemented with human epidermal growth factor, insulin, bovine pituitary extract, hydrocortisone, transferrin, epinephrine and GA-1000 (gentamicin–amphotericin) (Lonza, Basel, Switzerland). Wells and membranes were washed with 2 ml of media. Prior to the experiments, all membranes were sterilized by exposure to ultraviolet B light for 3 h on each side. During sterilization, the membranes were rotated 90° every 45 min. Upon completion of ultraviolet light sterilization, the membranes were placed in 6-well plates. Sterile stainless steel washers were used to weigh down the membranes to prevent them from floating to the surface. The media was changed after 24 h. Sampling was conducted after the HEK were 60% confluent. The HEK were assayed for viability using the metabolic marker MTT assay (3-[4,5-dimethyl-2-thiazol]-2,5-diphenyl-2H-tetrazolium bromide) [22]. Absorbance, directly proportional to cell viability, was determined spectrophotometrically at 550 nm in an ELISA plate reader (Multiskan RC, Labsystems, Helsinki, Finland). Membranes were moved to a new plate to prevent cells that had grown on the plate influencing the data. MTT viability cell proliferation assays were conducted in quadruplicate on diamond-like carbon-coated and as-prepared nanoporous alumina membrane. Gold-coated membranes and titanium-coated membranes were also examined for comparison purposes. HEK viability (normalized to media control) were statistically compared using ANOVA (SAS 9.1 for Windows, Cary, NC, USA). Multiple comparisons were made between different membrane types using the Student's *t*-test at $p < 0.05$.

Results and discussion

The diamond-like carbon-coated and as-prepared nanoporous alumina membranes were imaged using scanning probe microscope tapping mode, which avoided tip drag forces that are observed in scanning probe microscope contact mode. The atomic force micrographs of the as-prepared and diamond-like carbon-coated nanoporous alumina membranes are shown in figure 2. Monodisperse pore sizes, high porosities and smooth surfaces were observed. Biosensor membrane surfaces must

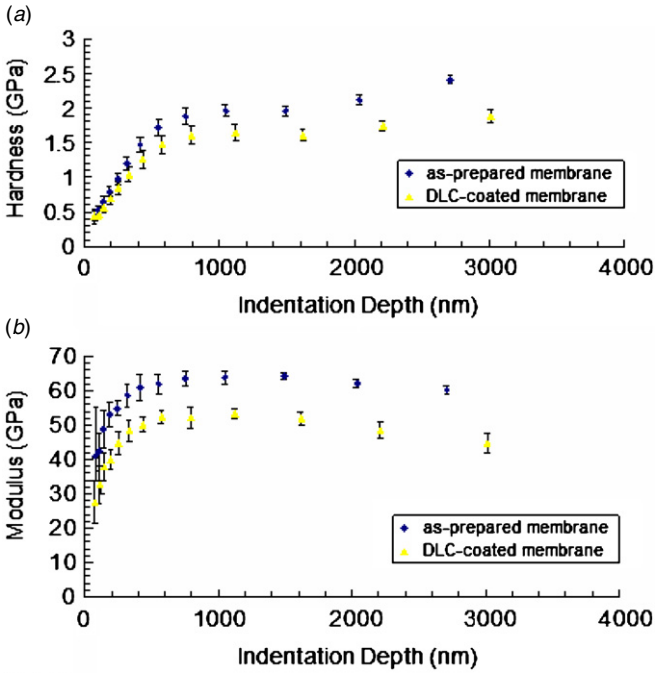

Figure 3. (*a*) Hardness versus indentation depth for as-prepared and diamond-like carbon-coated 100 nm pore size nanoporous alumina membranes. (*b*) Young's modulus versus indentation depth for as-prepared and diamond-like carbon-coated 100 nm pore size nanoporous alumina membranes.

be sufficiently porous to allow the sensor to rapidly respond to fluctuations in analyte concentration. The pore size can be controlled by altering the electrical field strength, processing temperature and electrolyte used in the anodization process. The diamond-like carbon-coated membrane exhibited slightly larger pore sizes than the as-prepared membrane. In pulsed laser deposition, a plume containing energetic ionic, atomic and molecular species (e.g., C^+ ions) is created by laser–target material interaction. These high energy species cause damage when they interact with the substrate. The energetic species sputter substrate atoms and form a 'collision region', which contains species from both the substrate and the plume [23–25]. The results of this study suggest that the increase in pore size observed in the diamond-like carbon-coated nanoporous alumina membranes results from localized heating of the nanoporous alumina membrane during the diamond-like carbon film deposition process.

Phase images of the as-prepared and diamond-like carbon-coated nanoporous membranes are shown in figures 2(*c*) and (*f*), respectively. Phase imaging involves plotting the phase lag of AFM cantilever oscillation when the cantilever is operated under tapping mode [26, 27]. The phase lag is sensitive to variations in material properties (e.g., modulus) and is insensitive to large height differences in a sample. Phase imaging may be used to obtain nanometer-scale data on the composition of a given material, including the presence of surface contaminants and the location of various component phases in a composite material. The uniform color in the phase contrast image of diamond-like carbon-coated nanoporous membrane suggests that no contaminants are present and that

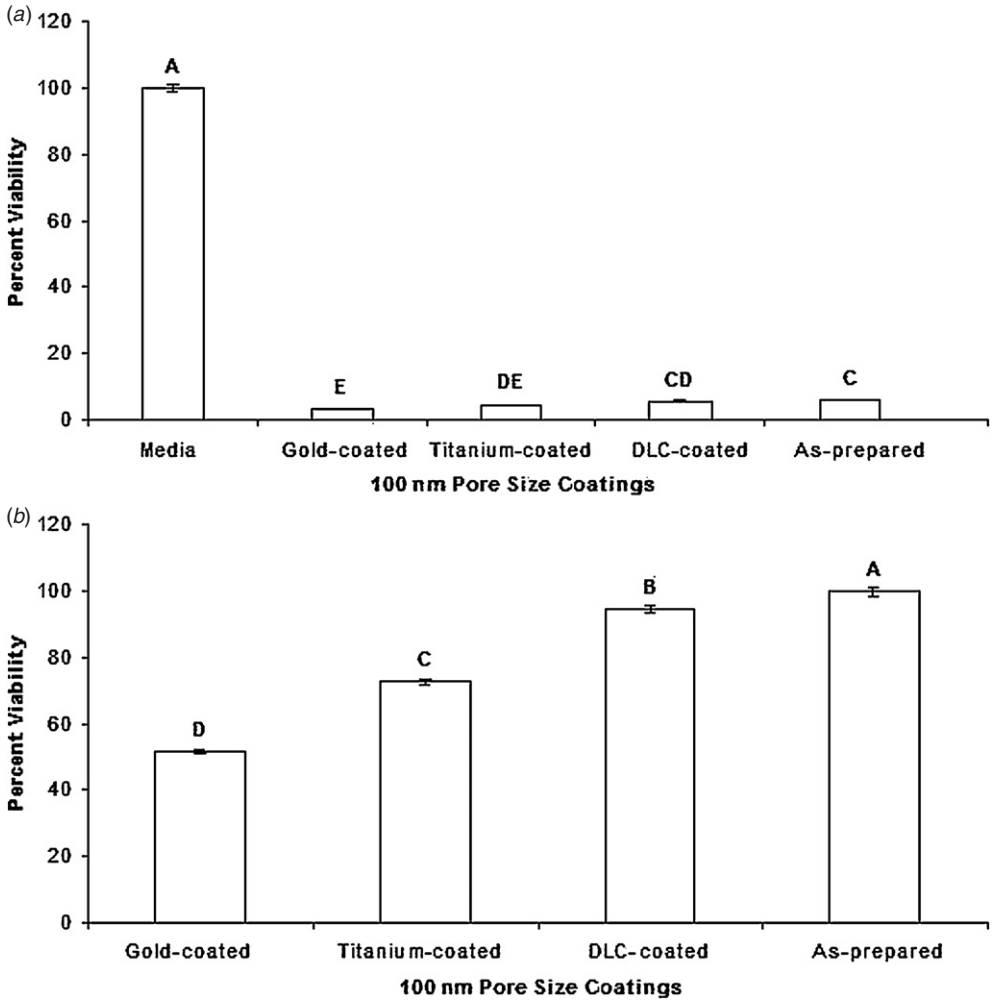

Figure 4. Twenty-four hour MTT viability assays for as-prepared, gold-coated, titanium-coated and diamond-like-carbon-coated 100 nm pore size membranes.

the diamond-like carbon film uniformly covers the surface of the nanoporous alumina membrane. The x-ray photoelectron spectrum for the diamond-like carbon-coated nanoporous alumina membrane revealed the presence of carbon, aluminum and oxygen.

Hardness and Young's modulus values for the diamond-like carbon-coated and as-prepared nanoporous alumina membranes are shown in figures 3(*a*) and (*b*), respectively. Average values were plotted versus the indentation depth. Error bars were used to indicate standard deviation values. Sokol *et al* used the thermal expansion method to measure the elastic modulus of the anodized aluminum with pores. They used the following formula:

$$E_0 = E_1(1 - p)^2 \quad (1)$$

to correlate Young's modulus of a porous material of a given composition with its nonporous counterpart. In this formula, $E_1 = 98.1$ GPa is the elastic modulus for nonporous anodic aluminum oxide and p is the pore volume per volume unit. According to this equation, membranes with larger pores exhibit lower modulus values. These results suggest that the lower hardness values and Young's modulus values observed in the diamond-like carbon-coated membranes result from larger pore sizes. Due to the brittleness of the as-prepared nanoporous alumina membranes and diamond-like carbon-coated nanoporous alumina membranes, it is anticipated that these membranes will require additional support or scaffolding for *in vivo* usage.

Twenty-four hour MTT viability assays for as-prepared, gold-coated, titanium-coated and diamond-like-carbon-coated 100 nm pore size membranes are shown in figure 4. The cells placed in the media control were significantly more viable than the cells placed on any of the membranes (figure 4(*a*)). Cells grown in media alone without any test materials demonstrated a statistically significant increase in viability compared to the membranes. Figure 4(*b*) depicts a comparison of MTT viability for coated and uncoated membranes, which shows a significant decrease in viability from diamond-like carbon-coated membranes to titanium-coated membranes to gold-coated membranes. It is interesting to note that the gold-coated membranes had the greatest significant decrease in viability compared to all other membranes, although gold is a noble metal that typically has little effects on cell growth proliferation [28]. Both gold and titanium have demonstrated good cell compatibility in previous studies [28]. These results suggest that the metal coatings formed galvanic couples with

metallic aluminum in the nanoporous alumina membranes, which accelerated aluminum ion release and lead to reduced viability rates. Previous studies have shown that diamond-like carbon thin films exhibit excellent compatibility with mouse peritoneal macrophages and mouse fibroblasts with no biochemical or morphological changes during *in vitro* studies [29]. In addition, Allen *et al* have shown that osteoblast-like cells exposed to diamond-like carbon did not demonstrate changes in alkaline phosphatase, type I collagen and osteocalcin production [30]. Linder *et al* have also shown that diamond-like carbon films do not affect macrophage activation and do not elicit an inflammatory response [31].

Conclusions

Novel biosensor membranes must exhibit appropriate structural, mechanical and biological properties for *in vivo* use. Scanning probe microscopy demonstrated that nanoporous alumina membranes exhibit monodisperse pore size and high porosity. Pulsed laser deposition was used to deposit atomically smooth diamond-like carbon thin films on the nanoporous alumina membranes. The diamond-like carbon-coated nanoporous alumina membranes exhibited mechanical properties slightly lower than those of as-prepared nanoporous alumina membranes due to their slightly larger pore sizes. In addition, diamond-like carbon-coated nanoporous alumina membranes demonstrated cell viability rates similar to those for as-prepared nanoporous alumina membranes. Future studies are underway to examine whether nanoporous alumina membranes modified with conformal coatings exhibit cell viability rates similar to nanoporous alumina membranes modified with line-of-sight coatings. Several medical uses for these novel materials are anticipated. For example, biomimetic ion transport functionality may be incorporated within the pores of the nanoporous membranes in order to modify nanopore diffusion characteristics. These pores would act similarly to the protein-based ion channels for electrical signaling in nerves and muscles.

Acknowledgments

The authors would like to thank K Evaul and AO Inman (Center for Chemical Toxicology Research and Pharmacokinetics, North Carolina State University) for their assistance with the MTT assays.

References

[1] Wisniewski N and Reichert M 2000 Methods for reducing biosensor membrane biofouling *Colloids Surf.* B **18** 197–219

[2] Elbicki J M and Weber S G 1989 Ultrafiltration of human-serum to determine the size of species that poison voltammetric electrodes *Biosensors* **4** 251–7

[3] Warkentin P, Walivaara B, Lundstrom I and Tengvall P 1994 Differential surface binding of albumin, immunoglobulin-G and fibrinogen *Biomaterials* **15** 786–95

[4] Shichiri M, Sakakida M, Nishida K and Shimoda S 1998 Enhanced, simplified glucose sensors: long-term clinical application of wearable artificial endocrine pancreas *Artif. Organs* **22** 32–42

[5] Reuben B G, Perl O, Morgan N L, Stratford P, Dudley L Y and Hawes C 1995 Phospholipid coatings for the prevention of membrane fouling *J. Chem. Technol. Biotechnol.* **63** 85–91

[6] Desai T A, Chu W H, Tu J K, Beattie G M, Hayek A and Ferrari M 1998 Microfabricated immunoisolating biocapsules *Biotechnol. Bioeng.* **57** 118–20

[7] Anderson S H C, Elliott H, Wallis D J, Canham L T and Powell J J 2003 Dissolution of different forms of partially porous silicon wafers under simulated physiological conditions *Phys. Status Solidi A* **197** 331–5

[8] Canham L T, Reeves C L, Loni A, Houlton M R, Newey J P, Simons A J and Cox T I 1997 Calcium phosphate nucleation on porous silicon: factors influencing kinetics in acellular simulated body fluids *Thin Solid Films* **297** 304–7

[9] Narayan R J *et al* 2007 Nanoporous hard carbon membranes for medical applications *J. Nanosci. Nanotechnol.* **7** 1486–93

[10] Matsuda H and Fukuda K 1995 Ordered metal nanohole arrays made by a two-step replication of honeycomb structures of anodic alumina *Science* **268** 1466–8

[11] Andara M, Agarwal A, Scholvin D, Gerhardt R A, Doraiswamy A, Jin C, Narayan R J, Shih C, Shih C, Lin S and Su Y 2006 Hemocompatibility of diamondlike carbon-metal composite thin films *Diamond Rel. Mater.* **15** 1941–8

[12] Narayan R J 2006 Laser processing of diamond-like carbon thin films for medical prostheses *Int. Mater. Rev.* **51** 128–43

[13] Narayan R J 2005 Pulsed laser deposition of functionally gradient tetrahedral amorphous carbon-metal nanocomposites *Diamond Rel. Mater.* **14** 319–30

[14] Narayan R J, Jin C, Doraiswamy A, Mihailescu I N, Jelinek M, Ovsianikov A, Chichkov B N and Chrisey D B 2005 Laser processing of advanced bioceramics *Adv. Eng. Mater.* **7** 1083–98

[15] Morrison M L, Buchanan R A, Liaw P K, Berry C J, Brigmon R, Riester L, Jin C and Narayan R J 2006 Electrochemical and antimicrobial properties of diamond-like carbon-metal composite films *Diamond Rel. Mater.* **15** 138–46

[16] Narayan R J and Scholvin D 2005 Synthesis and properties of nanostructured carbon-metal composite films *J. Vacuum Sci. Technol.* B **23** 1041–6

[17] Srinivasan S and Sawyer P N 1970 Role of surface charge of the blood vessel wall, blood cells, and prosthetic materials in intravascular thrombosis *J. Colloid Interface Sci.* **32** 456–63

[18] Monties J R, Dion I, Havlik P, Rouais F, Trinkl J and Baquey C 1997 Cora rotary pump for implantable left ventricular assist device: biomaterial aspects *Artif. Organs* **21** 730–4

[19] Jones M I, McColl I R, Grant D M, Parker K G and Parker T L 2000 Protein adsorption and platelet attachment and activation, on TiN, TiC, and DLC coatings on titanium for cardiovascular applications *J. Biomed. Mater. Res.* **52** 413–21

[20] Jones M I, McColl I R, Grant D M, Parker K G and Parker T L 1999 Haemocompatibility of DLC and TiC–TiN interlayers on titanium *Diamond Rel. Mater.* **8** 457–62

[21] Yu L J, Wang X, Wang X H and Liu X H 2000 Haemocompatibility of tetrahedral amorphous carbon films *Surf. Coat. Technol.* **128** 484–8

[22] Mossman T 1983 Rapid colorimetric assay for cellular growth and survival: application to proliferation and cytotoxicity assays *J. Immunologic. Methods* **65** 55–63

[23] Bulicz J, Morales de la Garza L and Fuentes S 1996 Chemical interaction of pulsed laster deposited Co with the MoS20001 surface *Surf. Sci.* **365** 411–21
[24] Bidin N, Qindeel R, Daud M Y and Bhatti K A 2007 Plasma splashing from Al and Cu materials induced by an Nd: YAG pulsed laser *Laser Phys.* **17** 1222–8
[25] Kukreja L M, Bhattacharya P, Ganguli T, Pandey B M and Rustagi K C 1998 Unusual growth modes in pulsed laser deposition of ZnSe thin films on GaAs *Mater. Sci. Forum* **287** 535–7
[26] Raghavan D, Gu X, Nguyen T, VanLandingham M and Karim A 2000 Mapping polymer heterogeneity by phase imaging and nanoindentation AFM *Macromolecules* **33** 2573–83
[27] Raghavan D, VanLandingham M, Gu X and Nguyen T 2000 Charactization of heterogeneous regions in polymer systems using tapping mode and force mode atomic force microscopy *Langmuir* **16** 9448–59
[28] Pistorius A and Willershausen B 2002 Biocompatibility of dental materials in two human cell lines *Eur. J. Med. Res.* **7** 81–8
[29] Thomson L A, Law F C, Rushton N and Franks J 1991 Biocompatibility of diamond-like carbon coating *Biomaterials* **12** 37–40
[30] Allen M, Myer B and Rushton N 2001 In vitro and *in vivo* investigations into the biocompatibility of diamond-like carbon (DLC) coatings for orthopedic applications *J. Biomed. Mater. Res.* **58** 319–28
[31] Linder S, Pinkowski W and Aepfelbacher M 2002 Adhesion, cytoskeletal architecture and activation status of primary human macrophages on a diamond-like carbon coated surface *Biomaterials* **23** 767–73